EUROfusion

EUROFUSION CP(15)04/34

K. Heinola et al.

Long Term Fuel Retention in JET ITER-Like Wall

(18th May 2015 – 22nd May 2015)
Aix-en-Provence, France

This work has been carried out within the framework of the EUROfusion Consortium and has received funding from the Euratom research and training programme 2014-2018 under grant agreement No 633053. The views and opinions expressed herein do not necessarily reflect those of the European Commission.

Long Term Fuel Retention in JET ITER-Like Wall

K. Heinola[1,2*], A. Widdowson[2], J. Likonen[3], E. Alves[4], A. Baron-Wiechec[2], N. Barradas[4], S. Brezinsek[5], N. Catarino[4], P. Coad[2], S. Koivuranta[3], S. Krat[6,7] G. F. Matthews[2], M. Mayer[6], P. Petersson[8] and JET Contributors[†]

EUROfusion Consortium, JET, Culham Science Centre, Abingdon, OX14 3DB, UK

[1]*University of Helsinki, PO Box 64, 00560 Helsinki, Finland*

[2]*CCFE, Culham Science Centre, Abingdon, OX14 3DB, UK*

[3]*VTT, PO Box 1000, 02044 VTT, Espoo, Finland*

[4]*Instituto Superior Tecnico, Instituto de Plasmas e Fusao Nuclear, Universidade de Lisboa, 1049-001 Lisboa, Portugal*

[5]*Forschungszentrum Julich GmbH, D-52425, Julich, Germany*

[6]*Max-Planck Institut fur Plasmaphysik, D-85748, Garching, Germany*

[7]*National Research Nuclear University MEPhl, 115409 Moscow, Russia and*

[8]*Royal Institute of Technology, SE-10044, Stockholm, Sweden*

[*] Corresponding author

Email: kalle.heinola@ccfe.ac.uk, *Tel*: +44(0) 1235 46 4478

[†] See the Appendix of F. Romanelli *et al.*, Proceedings of the 25th IAEA Fusion Energy Conference 2014, Saint Petersburg, Russia

Abstract

Post-mortem studies with Ion Beam Analysis, Thermal Desorption, and Secondary Ion Mass Spectrometry have been applied for investigating the long term fuel retention in the JET ITER-Like Wall components. The retention is mostly implantation dominated, but the highest retention values were found to correlate with the thickness of the deposited impurity layers. From the total amount of retained D fuel over half was detected in the divertor region. The majority of the retained D is on the top surface of inner divertor, whereas the least retention was measured in the main chamber on the mid-plane of inner wall limiter. The recessed areas of the inner wall may contribute significantly to the main chamber total retention. Thermal Desorption Spectroscopy analysis revealed the energetic T from DD reactions being implanted in the divertor. The total T inventory was assessed to be > 0.3 mg.

PACS numbers: 28.52.Fa 52.55.Fa 52.55.Pi 52.70.Nc 52.77.Dq

I. INTRODUCTION

Recycling and retention of the plasma fuel in the vessel first wall materials play a key role in economical operation of a fusion device. Radiological safety concerns set a limit on the hazardous hydrogen isotope tritium (T) inventory in the wall material. For ITER the present limit is 0.7 kg of T. The JET ITER-Like Wall (JET-ILW) project [1] allows us to investigate the plasma-surface interactions which can take place during ITER operation. The JET-ILW main chamber limiters are made out of bulk beryllium (Be) and the divertor region is comprised of bulk tungsten (W) tiles and W-coated carbon-fibre composite (CFC) tiles. Post-mortem analysis of the removed first wall components allows us to scrutinize the net effects of plasma-surface interactions. Removal and replacement of vessel wall tiles can be done only during dedicated shutdowns between JET experimental campaigns.

During the JET-ILW campaign 2011-2012 the deuterium (D) retention was studied with dedicated gas balance experiments for different plasma scenarios [2]. The outgassing of the retained D was monitored short term (in between pulses) as well as longer term (up to 2 days). JET-ILW gas balance measurements showed a fuel retention which was $10-20$ times smaller than what was measured with the JET all-Carbon (JET-C) wall campaign 2007-2009. The first post-mortem assessment for fuel retention in JET-ILW after the 2011-2012 experimental campaign agreed with the gas balance results showing a reduction by a factor of 18 when compared to JET-C [3]. Present work expands that work by providing fully analyzed results for the main chamber, extending the analyzed region to cover both the inner and the outer wall in full, and providing the first assessment of the T total inventory in the divertor. The fuel detected in these analyses shows the net retention of D beyond the long-term outgassing, and the results map the retention distribution in the vessel.

II. EXPERIMENTAL METHODS

During JET-ILW 2011-2012 campaign approximately 1.67×10^{26} D atoms were puffed in the machine [4] in ~ 3000 discharges. The post-campaign, or post-mortem D concentrations were determined from selected JET-ILW first wall armour tiles removed from the vessel during the shutdown 2012-2013. The tiles were a representative selection from the main chamber first wall limiters (Fig. 1 and Ref. [5]): the upper region, mid-plane and lower region of Inner Wall Guard Limiters (IWGL) and Outer Poloidal Limiters (OPL), as well as tiles from the divertor (inner and

outer divertor). Samples from the central part of the divertor (Tile 5) have been removed in the beginning of 2015, and the first results are scheduled to be available in the beginning of 2016. In addition to the main chamber limiters, samples from the recessed inner wall limiters and from the inner wall were collected for analysis (Fig. 2). The recessed outer wall retention has been assessed with results from the main chamber wall mirror analyses [6].

A special marker coating was applied to the selected first wall tiles prior their installation in 2010 for measuring the tile erosion/deposition accurately after the first JET-ILW campaign. The bulk Be marker tiles of the main chamber have a Ni-Be layered coating. The W-coated CFC divertor marker tiles have a Mo coating as a marker interlayer, except Tile 3 which has the Mo layer as the plasma-facing coating. The recessed inner wall limiter tiles are either W-coated CFC, or Be-coated Inconel tiles and without any marker coating. The inner wall is protected with Inner Wall Cladding (IWC) tiles, which are Inconel or CFC tiles coated with W or Be, respectively. The removed IWC samples were W/Be coated inserts being installed to IWC tiles for easy replacement and analysis (details in Ref. [7]).

Post-mortem studies were carried out with Ion Beam Analysis (IBA), Thermal Desorption Spectroscopy (TDS), and Secondary Ion Mass Spetrcometry (SIMS) methods. In IBA, the Nuclear Reaction Analysis (NRA) was used for determining the deuterium concentrations via the $D(^3He,p)^4He$ nuclear reaction. With NRA also the Be and C impurity concentrations were evaluated with the $^9Be(^3He, p)^{11}B$ and $^{12}C(^3He, p)^{14}N$ reactions, respectively. The energy used for the ^3He beam was either 2.3 MeV, or 4.5 MeV. The use of higher ^3He energy 4.5 MeV enables D and Be concentration analysis to larger depths, and improves the C detection efficiency as the reaction cross-section increases with projectile ion energy. Elastic Backscattering (EBS) and Particle Induced X-ray Emission (PIXE) were used in conjunction with 2.3 MeV ^3He beam for detecting Be and heavier elements. The 2.3 MeV NRA, EBS and PIXE results were fitted with WiNDF data furnace software package [8], and their experimental setups are described in detail in Refs. [5, 9].

The main chamber bulk Be samples (IWGL, OPL, DP), and the inner divertor were analyzed with 2.3 MeV NRA jointly with EBS and PIXE, and results were fitted parallelly with WiNDF. The divertor tiles were studied fully with 4.5 MeV NRA [7, 10] and analysed with SIMNRA package [11]. Also, Elastic Recoil Detection Analysis (ERDA) was performed for studying the co-deposits found at the divertor [12]. SIMS analysis was performed for studying the D concentrations both on the inner and on the outer divertor samples. Details for the SIMS setup are presented in Ref. [13]. The SIMS results were calibrated with D reference samples, which were prepared by implanting

60 keV/D_2 into polycrystalline W (see details in Ref.[14]). The retained D in the implantation-induced defects was determined with ERDA at University of Helsinki, Finland, and was found to be 3.47×10^{16} at./cm^2.

TDS was applied to a number of divertor tile samples, and bulk Be main chamber samples [15, 16]. The analysis was done in an ultra-high vacuum (UHV) system with a starting pressure of $\lesssim 1 \times 10^{-9}$ mbar. Samples were annealed with linear ramp rates (10 K/min or 5 K/min) from room temperature (RT) up to 1000°C. The released gases were measured with a line-of-sight quadrupole mass spectrometer as a function of time and annealing temperature. The TDS data was collected for mass-to-charge ratios corresponding to various molecules, e.g. H_2, HD, D_2, DT, T_2 and Be. The D signal was calibrated with the same D-implanted reference samples described previously.

The IBA for main wall tiles was performed using each individual bulk Be tile as a sample. The divertor tiles were cored into small-sized samples by using a hollow drill (diameter 17 mm), which were then analysed with SIMS and NRA [13]. An additional set of divertor samples were cored to be used with TDS. The topmost part of the TDS samples were further sliced horizontally into two pieces. The resulting TDS depth profile represents depths of 0 to 1 mm (surface coating sample) and 1.5 mm to 2.5 mm (bulk CFC sample). Additionally, samples from the main chamber bulk Be tiles were cut for TDS analysis [17]. The 12×12 mm^2 and 2 mm thick bulk Be samples were cut with a bandsaw from the tile castellations while keeping the castellation temperature below 55°C.

Finally, although the analysis methods used in this work provide accurate results locally (uncertainty $\lesssim 6\%$), the biggest uncertainty arises from the assumption of toroidal symmetries used in the extrapolation of the results to cover the full JET first wall surface area.

III. RESULTS AND DISCUSSION

A. Main chamber

1. Upper Dump Plates

In earlier work it was shown that the plasma-facing surfaces of the upper dump plate (DP) tiles were modified due to melting and arcing, which e.g. induced droplets of molten Be being ejected to the outer divertor [5, 18]. These strong interactions with plasma and DP region were mostly taking place before the active use of JET's Disruption Mitigation Valve protection system.

DP tile (identification 2B2C) was analysed with NRA and EBS providing information on the

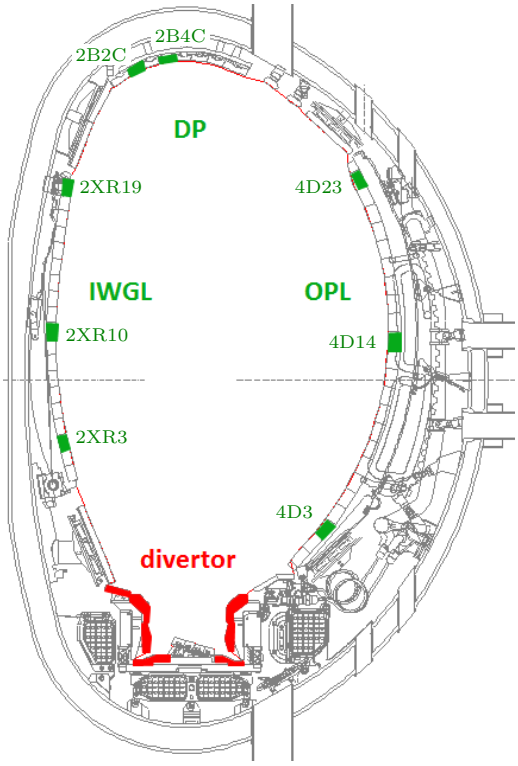

FIG. 1: (Color online) Cross-section of JET-ILW vessel showing locations of the removed first wall tiles for analysis. Main chamber components (DP, IWGL, OPL) are of bulk Be (highlighted in green). Divertor tiles used in the present study were W-coated CFC tiles (red).

thickness of the residual Ni-Be coating and on fuel retention. 21 measurement points in toroidal direction were used to cover the DP tile surface analysis. Each individual measurement point was then analysed with WiNDF and the impurity quantities and concentration profiles were determined respectively. The mean D concentration value and its deviation obtained was $(3.4 \pm 1.2) \times 10^{17}$ at./cm^2. Integrating over the whole upper DP region yields a retention value of 2.1×10^{22} D atoms.

2. Outer Wall: Limiters and recessed wall

Outer Poloidal Limiter (OPL) tiles used for post-mortem analysis were removed from the upper region, mid-plane and from the lower outer wall region (identification 4D23, 4D14 and 4D3, respectively, shown in Fig. 1). Each tile was measured with NRA, EBS and PIXE using 52 measurement points across the tile in the toroidal direction. The tiles showed thinning of the Be layer

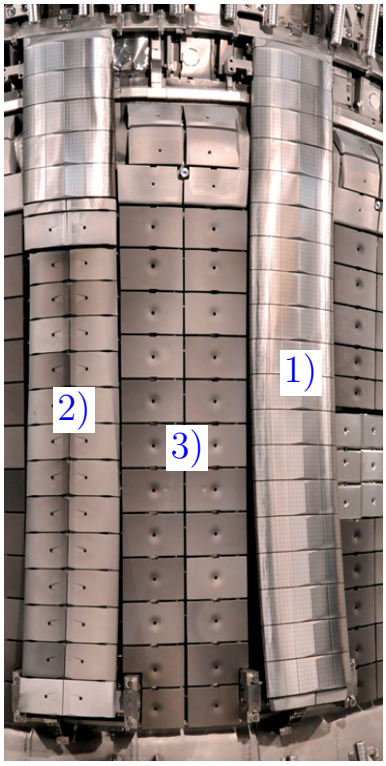

FIG. 2: (Color online) Close-up of the JET-ILW inner wall components used in present analyses: 1) IWGL, 2) recessed inner limiter, and 3) inner wall consisting of IWC tiles. The recessed limiters are either W-coated CFC or Be-coated Inconel and ~ 2.5 cm further away from the plasma as the bulk Be IWGLs. The IWC tiles are W-coated CFC or Be-coated Inconel tiles.

in the centre part of the tile [19]. The centre region was neighboured by some deposited Be which extends to the far ends of the tile. The lower region OPL tile (4D3) analysis results to an integrated D total retention value of 1.50×10^{20} D atoms. A higher retention value 2.81×10^{20} D atoms was obtained for the mid-plane tile (4D14). The result for the upper region tile (4D23) was 1.21×10^{20} D atoms. Assuming parabolic symmetry for the D retention along the OPL beam in the poloidal direction and interpolating the aforementioned retention values, an integrated value for the D retention in one OPL beam can be obtained 5.02×10^{21} D atoms. In JET there are smaller limiters near the antennas which are likewise made out of bulk Be. Taking into account the difference in areal surfaces of an OPL and an antenna limiter, a D retention value for one antenna limiter can be assessed as 2.41×10^{21} D atoms. Multiplying the OPL and antenna limiter D values by their corresponding number of limiters to cover the whole machine (9 and 3, respectively), yields a global retention of 5.2×10^{22} D atoms on the outer wall limiters.

An earlier work presented impurity deposition and fuel retention results from mirror samples positioned in the main chamber [6]. The worst case result for the retention in the recessed outer wall was found to be $\sim 2 \times 10^{16}$ D at./cm^2. By multiplying that value with the recessed outer wall surface area, a total retention value can be obtained as 8.8×10^{21} D atoms. Retention to the recessed outer wall does not have a contribution to the global retention despite the very high surface area.

3. Inner Wall: IWGL, recessed limiters and IWC

IWGL tiles used in the present study were removed from the upper region, mid-plane and lower region of the inner wall (identification 2XR19, 2XR10 and 2XR3, respectively, shown in Fig. 1). As was with the OPL tiles, the IBA analysis for IWGL tiles was done in the toroidal direction of the tiles.

The D retention values obtained for upper, mid-plane and lower IWGL tiles were 8.17×10^{19}, 6.76×10^{19} and 8.14×10^{19} D atoms, respectively. The lowest D retention is measured at the mid-plane with the highest erosion rate as was previously shown with tile surface profilometry [18]. Assuming a parabolic retention symmetry in the poloidal direction and interpolating the retention values along the IWGL beam, a total D retention value of 1.4×10^{21} D atoms per one IWGL beam is obtained. Multiplying this by the number of IWGL beams (10) in the machine gives a global IWGL D retention value of 1.4×10^{22} D atoms.

The recessed inner wall limiters (Fig. 2) are ~ 2.5 cm further away from the plasma as the surface of IWGL tiles, and hence face less direct interactions with the ions in the plasma. A W-coated recessed limiter tile assembly was removed from the limiter mid-plane (identification of sub-tiles 7Z12R and 7Z12L) for IBA analysis. Assembly tiles were measured with 2.3 MeV NRA in the toroidal direction, and the results were calibrated against experimental and WiNDF data obtained for IWGL mid-plane (2XR10). The analysis revealed a nearly homogeneous D distribution along the tile assembly with 9.3×10^{19} D atoms. No Be was detected. Multiplying by the number of tile assemblies in JET vessel (both W-coated CFC and Be-coated Inconel) a total recessed limiter inventory of 1.1×10^{22} D atoms is obtained. It is noteworthy that the recessed limiter D inventory has the same order of magnitude as the IWGL D inventory even though the IWGL surface area is a factor of ~ 1.6 higher.

The inner wall D inventory has been assessed by analyzing special probes which were inserted

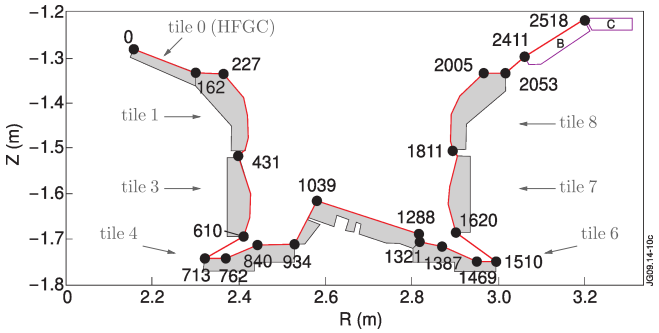

FIG. 3: (Color online) The divertor S coordinate system showing poloidal trajectory following the tile surfaces. The tile 1 apron is between S coordinates 162 mm and 227 mm.

to the IWC tiles (Fig. 2). Details of the locations of the IWC tiles with inserts and the analysis results can be found in Ref. [7]. To summarize, the results of D concetrations in Be-coated Inconel and W-coated CFC IWC tiles were rather identical ($\sim 2 \times 10^{17}$ at./cm^2 and $\sim 9 \times 10^{16}$ at./cm^2, respectively) in both toroidal and poloidal directions. Integrating over corresponding inner wall areas a total inventory is obtained 1.7×10^{21} D atoms.

The results for the recessed limiters and inner wall show, that these areas have a significant contribution to the total inner wall D inventory. Since the recessed areas do not interact with the plasma ions, the fuel accumulation is due to implantation of the charge exchange (CX) neutrals escaping the plasma. It has been previously shown, that the IWC are is a net erosion zone due to the CX neutrals [**?**].

B. Divertor

1. Deuterium distribution

NRA with 4.5 MeV ^{3}He, and SIMS were used for determining the D concentrations in the divertor [10, 18]. Additionally, the inner divertor samples were analysed with 2.3 MeV NRA combined with EBS and PIXE. The resulted IBA values are presented together with TDS results in Fig. 4. The measurement points form a poloidal distribution along the divertor. For locating the analysis points an S coordinate system is used and presented in Fig. 3. Results from Tiles 0, 1, 3, and 4 comprise the inner divertor, and Tiles 6, 7, and 8 the outer divertor.

Divertor D retention trend shows clearly that most of the retained D is on the inner divertor.

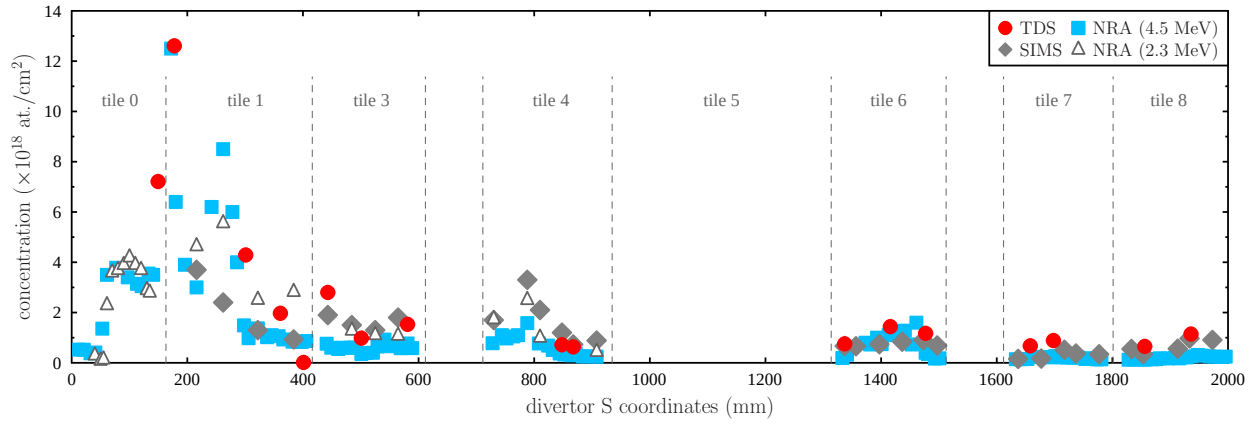

FIG. 4: (Color online) The poloidal distribution of retained D in the JET-ILW divertor tiles as measured with TDS, SIMS and NRA (with 2.3 and 4.5 MeV). D concentration is presented as a function of S coordinates. The divertor tile positions at corresponding S coordinates are separated with dashed lines.

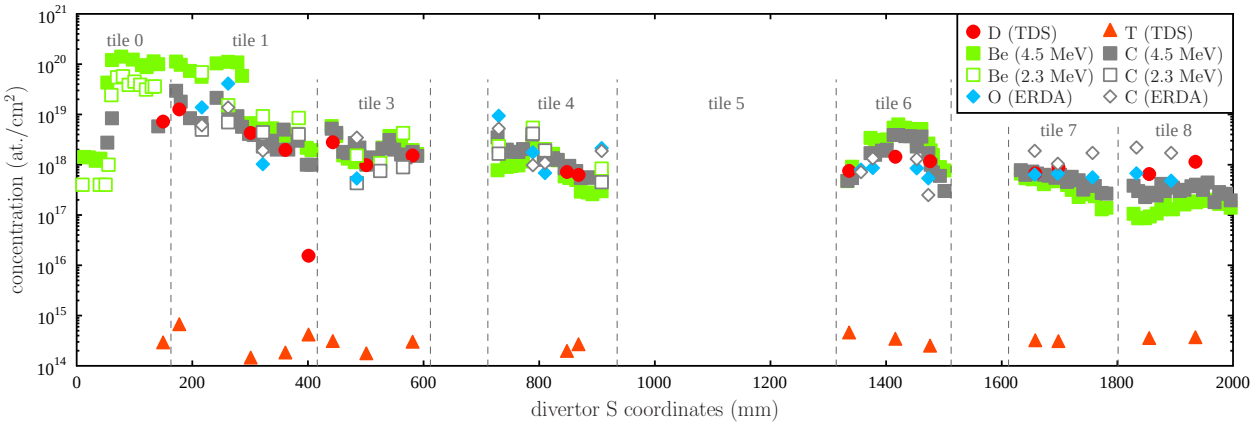

FIG. 5: (Color online) The poloidal distribution of retained D and T as measured with TDS. The T values are found to be low ($< 10^{15}$ at./cm^2) along the divertor, and originate from implanted T from DD reactions. Also shown the poloidal Be, C and O concentrations.

Local variation is observed in the values obtained with different analysis methods. These may be due to toroidal variation of D concentration, and surface roughness effects. Moreover, it has been shown recently that local nonuniformity of the D surface distribution takes place in the analyzed divertor samples [20, 21]. Averaging the D retention values per tile presented in Fig. 4 and integrating over all the divertor tiles in toroidal direction gives total D concentration values of 1.7×10^{23} and 3.9×10^{22} D atoms for the inner and outer divertor, respectively. Over 72% of the inner divertor D retention takes place on Tile 0 (HFGC) and Tile 1. This correlates with the

TABLE I: Summary of the retained D total amounts from JET-ILW 2010 – 2012 campaign.

JET vessel component	number of D atoms
Upper Dump Plates	2.1×10^{22}
Outer Poloidal Limiters	5.2×10^{22}
−outer wall‡	8.8×10^{21}
Inner Wall Guard Limiters	1.4×10^{22}
−recessed limiters‡	1.1×10^{22}
−inner wall (IWC tiles)‡	1.7×10^{22}
Divertor, total	2.1×10^{23}
−inner divertor (incl. Tile 0)	1.7×10^{23}
−Tile 0 and Tile 1	1.2×10^{23}
−outer divertor	3.9×10^{22}
−Tile 5	not measured
Remote areas, total	4.2×10^{22}
−inner louvre	2.0×10^{22}
−outer louvre	2.2×10^{22}

‡ not included in global fuel retention rate assessment (see text for details)

thickest deposition measured from that region. Fig. 5 presents the results of the divertor deposited layers. The deposition structure and mixing of the deposited materials have been studied experimentally [10, 19, 21] and computationally [22]. From the divertor results it is ambiguous whether the D retention is composition dependent of the deposited layer. Some correlation of D retention is with the thickness of the deposited layer on the inner divertor. The outer divertor deposited layers do not vary as much as the layers on the inner divertor.

Passive diagnostic Louvre Clips (LC) were installed in divertor pump ducts for monitoring

deposition on the remote cold regions in the inner and outer divertor (areas between Tile 3 and 4 and Tile 6 and 7, Fig. 3). The amount of retained D on the inner and outer LC was $(3.0 \pm 1.7) \times 10^{18}$ at./cm^2 and $(1.9 \pm 0.8) \times 10^{18}$ at./cm^2, respectively.

The integrated D concentration values from TDS are presented in Fig. 4 and Fig. 5. In addition to the 1 mm thick samples of the W-coated surface, bulk CFC samples were prepared from every divertor tile. The CFC sample depth corresponds to 1.5 mm from the tile surface. The TDS analyses with the CFC samples showed a general D concentration of $\lesssim 10^{15}$ at./cm^2 when annealed to 1000°C [15]. At this moment, it remains unclear whether this low value is a real effect of D diffusion, or it merely shows the limitation of the sample preparation by coring.

The D_2 desorption spectra for divertor samples are fairly broad and consist mostly of two main desorption peaks from which the first one comprises of two sub-peaks [15, 16]. The desorption was observed to start typically at ~ 80°C in UHV.

2. Tritium retention

A small T_2 signal was recorded with TDS at low temperatures, but a clear T_2 outgassing took place at high temperatures $\sim 700 - 800$°C. The low temperature T_2 peak may be due to thermalized T being co-deposited on tile surfaces. It is highly plausible that the high temperature T_2 release is due to energetic T being implanted into the samples. Recent results with ASCOT Monte Carlo simulations show that 99% of T being formed in JET DD plasma leave the plasma with an energy of 1 MeV (Fig. **??**) [23]. These energetic implantations produce deep T concentrations and implantation-induced defects with strong binding energies, i.e. high temperatures are required for the T being released from the sample. The T poloidal distribution along the divertor does not show variation as was measured for the D. A mean value for divertor T concentration can be obtained $(2.9 \pm 1.1) \times 10^{14}$ at./cm^2. This results into $(5.2 \pm 2.1) \times 10^{19}$ T atoms (0.3 mg) when integrated over the whole divertor (excluding Tile 5). Additionally, at high temperatures $\gtrsim 800$°C the desorption of Be was initiated. Since bulk Be is having a melting point at ~ 1200°C, it is concluded that the observed signal is due to the evaporation of the Be deposits from the sample surface. As the Be desorption takes place at the high end of the annealing profile, total quantities were not concluded within this work.

IV. SUMMARY AND CONCLUSIONS

Table I summarizes the present results on global D retention of JET-ILW as measured from the first wall and recessed wall areas. Results are obtained by analysing a poloidal selection of first wall tiles, and probes from selected wall areas. Global values are calculated by assuming a toroidal symmetry in JET vessel. The largest uncertainty in the global values arises from the assumption of toroidal symmetry of the locally obtained results, which leads to the extrapolation to cover the full first wall surface area.

In JET-ILW, the D retention process is mostly implantation dominant, whereas for JET-C the D was found in massive C deposits, which covered large areas of the first wall. However, in JET-ILW the highest retention values were measured from regions with highest deposition. Lower retention was obtained in areas with thin impurity layers or where implantation might be the main retention mechanism. Moreover, it was found that the inner wall recessed areas contribute largely to the main chamber retention, whereas the outer wall recessed area has an insignificant contribution despite its large surface area.

During the 2011-2012 experimental campaign approx. 1.67×10^{26} D atoms were puffed into JET [4]. The post-mortem analyses of the present work map the distribution of the 3.7×10^{23} retained D atoms, which corresponds to $\sim 0.2\%$ or 1.2g of retained D. This results to a global retention rate of 5.5×10^{18} D/s when normalised to 6.8×10^{4} s operational time of the 2010-2012 JET-ILW campaign.

Using the JET-ILW limiter (6h) and divertor (13h) plasma configuration times results in retention rates 4.0×10^{18} D/s and 5.3×10^{18} D/s for the main chamber and divertor, respectively. For comparison, the JET-C 2007-2009 campaign main chamber (12h) [24, 25] and divertor (33h) [25, 26] retention rates are 1.9×10^{19} D/s and 1.3×10^{20} D/s. The JET-C 2007-2009 results have been re-assessed [25] and e.g. include retention in the remote areas. The resulted JET-C global retention in 2007-2009 is 1.0×10^{20} D/s, which is by a factor ~ 18 higher than the corresponding JET-ILW 2010-2012 result.

No cleaning pulses for removing fuel from the wall were preformed in the end of JET-ILW 2011-2012. However, the hydrogen isotope exchange effect studied with gas balance[27], and Ion Cyclotron Wall Conditioning experiments[28] suggest a limited D reservoir being accessible for the fuel removal (3.5×10^{22} and 7.0×10^{22} D atoms, respectively). Hence, the reduction of fuel retention due to isotopic exchange effects can be assessed to be $\sim 10\%$ for a typical JET-ILW

campaign.

The T distribution on the divertor was determined with TDS. Results show that some T is released at low temperatures, but the major desorption starts at ~ 700 degC. The high temperature release can be concluded to be originating from energetic 1 MeV T formed in DD plasmas. Further studies are required for more detailed assessment for the T retention mechanism in JET-ILW.

Acknowledgments

The assistance of K. Mizohata in preparation and analysis of the D calibration samples at the University of Helsinki, Finland, is highly acknowledged.

This work has been carried out within the framework of the EUROfusion Consortium and has received funding from the Euratom research and training programme 2014-2018 under grant agreement No 633053. The views and opinions expressed herein do not necessarily reflect those of the European Commission.

[1] G. F. Matthews, P. Edwards, T. Hirai, M. Kear, A. Lioure, P. Lomas, A. Loving, C. Lungu, H. Maier, P. Mertens, et al., Phys. Scripta **T128**, 137 (2007).

[2] S. Brezinsek, T. Loarer, V. Philipps, H. Esser, S. GrÃijnhagen, R. Smith, R. Felton, J. Banks, P. Belo, A. Boboc, et al., Nucl. Fusion. **53**, 083023 (2013).

[3] K. Heinola, A. Widdowsona, J. Likonen, E. Alves, A. Baron-Wiechec, N. Barradas, S. Brezinsek, N. Catarino, P. Coad, S. Koivuranta, et al., J. Nucl. Mater. (2014), in press.

[4] V. Philipps, private communication (2014).

[5] A. Widdowson, E. Alves, C. F. Ayres, A. Baron-Wiechec, S. Brezinsek, N. Catarino, J. P. Coad, K. Heinola, J. Likonen, G. F. Matthews, et al., Phys. Scripta **T159**, 014010 (2014).

[6] D. Ivanova, M. Rubel, A. Widdowson, P. Petersson, J. Likonen, L. Marot, E. Alves, A. Garcia-Carrasco, and G. Pintsuk, Phys. Scripta **T159**, 014011 (2014).

[7] S. Krat, Y. Gasparyan, A. Pisarev, I. Bykov, M. Mayer, G. de Saint Aubin, M. Balden, C. P. Lungu, and A. Widdowson, J. Nucl. Mater. **456**, 106 (2015).

[8] N. P. Barradas and C. Jeynes, Nucl. Instr. Meth. Phys. Res. B **266**, 1875 (2008).

[9] J. P. Coad, E. Alves, N. P. Barradas, A. Baron-Wiechec, N. Catarino, K. Heinola, J. Likonen, M. Mayer, G. F. Matthews, P. Petersson, et al., Phys. Scripta **T159**, 014012 (2014).

[10] S. Krat, M. Mayer, and et al., to be published (2015).

[11] J. B. J.F. Ziegler and M. Ziegler, *SIMNRA User's Guide 6.05* (Max-Planck-Institut für Plasmaphysik, Garching, Germany, 2009), http://home.rzg.mpg.de/ mam/index.html.

[12] P. Petersson, H. Bergsåker, I. Bykov, G. Possnert, J. Likonen, J. Linke, S. Koivuranta, A. Widdowson, H. G. Esser, and M. Rubel, J. Nucl. Mater. (2014).

[13] J. Likonen, E. Alves, A. Baron-Wiechec, S. Brezinsek, J. P. Coad, A. Hakola, K. Heinola, S. Koivuranta, G. F. Matthews, P. Petersson, et al., Phys. Scripta **T159**, 014016 (2014).

[14] K. Heinola, T. Ahlgren, E. Vainonen-Ahlgren, J. Likonen, and J. Keinonen, Phys. Scripta **T128**, 91 (2007).

[15] J. Likonen, K. Heinola, A. D. Backer, S. Koivurant, A. Hakola, C. F. Ayres, A. Baron-Wiechec, P. Coad, G. F. Matthews, and A. Widdowson, PFMC-15 proceedings (2015).

[16] A. Baron-Wiechec, P. Coad, K. Heinola, J. Likonen, G. F. Matthews, and A. Widdowson, PFMC-15 proceedings (2015).

[17] A. Widdowson, A. Baron-Wiechec, J. P. Coad, K. Heinola, J. Likonen, G. F. Matthews, and M. Rubel, PFMC-15 proceedings (2015).

[18] K. Heinola, C. F. Ayres, A. Baron-Wiechec, J. P. Coad, J. Likonen, G. F. Matthews, and A. Widdowson, Phys. Scripta **T159**, 014013 (2014).

[19] A. Baron-Wiechec, A. Widdowson, E. Alves, C. F. Ayres, N. P. Barradas, S. Brezinsek, J. P. Coad, N. Catarino, K. Heinola, J. Likonen, et al., J. Nucl. Mater. (2015), in press.

[20] H. Bergsåker, P. Petersson, I. Bykov, G. Possnert, J. Likonen, S. Koivuranta, J. P. Coad, W. van Renterghem, I. Uytdenhouven, and A. Widdowson, J. Nucl. Mater. (2014), in press.

[21] H. Bergsåker, I. Bykov, Y. Zhou, P. Petersson, G. Possnert, J. Likonen, S. Koivuranta, , and A. Widdowson, PFMC-15 proceedings (2015).

[22] A. Lasa, K. Heinola, and K. Nordlund, Nucl. Fusion. **54**, 083001 (2014).

[23] T. Koskela, private communication (2015).

[24] S. Koivuranta, J. Likonen, A. Hakola, J. P. Coad, A. Widdowson, D. E. Hole, and M. Rubel, Phys. Scripta **T159**, 014052 (2014).

[25] J. Likonen, private communication (2014).

[26] S. Koivuranta, J. Likonen, A. Hakola, J. P. Coad, A. Widdowson, D. E. Hole, and M. Rubel, J. Nucl.

Mater. **438**, S735 (2013).

[27] T. Loarer, S. Brezinsek, V. Philipps, S. Romanelli-Gruenhagen, D. Alves, I. Carvalho, D. Douai, H. Esser, R. Felton, D. Frigione, et al., J. Nucl. Mater. (2014), in press.

[28] T. Wauters, D. Douai, D. Kogut, A. Lyssoivan, S. Brezinsek, E. Belonohy, T. Blackman, V. Bobkov, K. Crombe, A. Drenik, et al., J. Nucl. Mater. (2015), in press.